# Measurements of the center-of-mass energies at BESIII via the di-muon process*

M. Ablikim(麦迪娜)[1] M. N. Achasov[9,f] X. C. Ai(艾小聪)[1] O. Albayrak[5] M. Albrecht[4] D. J. Ambrose[44] A. Amoroso[49A,49C] F. F. An(安芬芬)[1] Q. An(安琪)[46,a] J. Z. Bai(白景芝)[1] R. Baldini Ferroli[20A] Y. Ban(班勇)[31] D. W. Bennett[19] J. V. Bennett[5] M. Bertani[20A] D. Bettoni[21A] J. M. Bian(边渐鸣)[43] F. Bianchi[49A,49C] E. Boger[23,d] I. Boyko[23] R. A. Briere[5] H. Cai(蔡浩)[51] X. Cai(蔡啸)[1,a] O. Cakir[40A,b] A. Calcaterra[20A] G. F. Cao(曹国富)[1] S. A. Cetin[40B] J. F. Chang(常劲帆)[1,a] G. Chelkov[23,d,e] G. Chen(陈刚)[1] H. S. Chen(陈和生)[1] H. Y. Chen(陈海云)[2] J. C. Chen(陈江川)[1] M. L. Chen(陈玛丽)[1,a] S. J. Chen(陈申见)[29] X. Chen(谌炫)[1,a] X. R. Chen(陈旭荣)[26] Y. B. Chen(陈元柏)[1,a] H. P. Cheng(程和平)[17] X. K. Chu(褚新坤)[31] G. Cibinetto[21A] H. L. Dai(代洪亮)[1,a] J. P. Dai(代建平)[34] A. Dbeyssi[14] D. Dedovich[23] Z. Y. Deng(邓子艳)[1] A. Denig[22] I. Denysenko[23] M. Destefanis[49A,49C] F. De Mori[49A,49C] Y. Ding(丁勇)[27] C. Dong(董超)[30] J. Dong(董静)[1,a] L. Y. Dong(董燎原)[1] M. Y. Dong(董明义)[1,a] S. X. Du(杜书先)[53] P. F. Duan(段鹏飞)[1] J. Z. Fan(范荆州)[39] J. Fang(方建)[1,a] S. S. Fang(房双世)[1] X. Fang(方馨)[46,a] Y. Fang(方易)[1] L. Fava[49B,49C] F. Feldbauer[22] G. Felici[20A] C. Q. Feng(封常青)[46,a] E. Fioravanti[21A] M. Fritsch[14,22] C. D. Fu(傅成栋)[1] Q. Gao(高清)[1] X. L. Gao(高鑫磊)[46,a] X. Y. Gao(高旭阳)[2] Y. Gao(高原宁)[39] Z. Gao(高榛)[46,a] I. Garzia[21A] K. Goetzen[10] W. X. Gong(龚文煊)[1,a] W. Gradl[22] M. Greco[49A,49C] M. H. Gu(顾旻皓)[1,a] Y. T. Gu(顾运厅)[12] Y. H. Guan(管颖慧)[1] A. Q. Guo(郭爱强)[1] L. B. Guo(郭立波)[28] Y. Guo(郭玥)[1] Y. P. Guo(郭玉萍)[22] Z. Haddadi[25] A. Hafner[22] S. Han(韩爽)[51] X. Q. Hao(郝喜庆)[15] F. A. Harris[42] K. L. He(何康林)[1] T. Held[4] Y. K. Heng(衡月昆)[1,a] Z. L. Hou(侯治龙)[1] C. Hu(胡琛)[28] H. M. Hu(胡海明)[1] J. F. Hu(胡继峰)[49A,49C] T. Hu(胡涛)[1,a] Y. Hu(胡誉)[1] G. M. Huang(黄光明)[6] G. S. Huang(黄光顺)[46,a] J. S. Huang(黄金书)[15] X. T. Huang(黄性涛)[33] Y. Huang(黄勇)[29] T. Hussain[48] Q. Ji(纪全)[1] Q. P. Ji(姬清平)[30] X. B. Ji(季晓斌)[1] X. L. Ji(季筱璐)[1,a] L. W. Jiang(姜鲁文)[51] X. S. Jiang(江晓山)[1,a] X. Y. Jiang(蒋兴雨)[30] J. B. Jiao(焦健斌)[33] Z. Jiao(焦铮)[17] D. P. Jin(金大鹏)[1,a] S. Jin(金山)[1] T. Johansson[50] A. Julin[43] N. Kalantar-Nayestanaki[25] X. L. Kang(康晓琳)[1] X. S. Kang(康晓珅)[30] M. Kavatsyuk[25] B. C. Ke[5] P. Kiese[22] R. Kliemt[14] B. Kloss[22] O. B. Kolcu[40B,i] B. Kopf[4] M. Kornicer[42] W. Kühn[24] A. Kupsc[50] J. S. Lange[24] M. Lara[19] P. Larin[14] C. Leng[49C] C. Li(李翠)[50] Cheng Li(李澄)[46,a] D. M. Li(李德民)[53] F. Li(李飞)[1,a] F. Y. Li(李峰云)[31] G. Li(李刚)[1] H. B. Li(李海波)[1] J. C. Li(李家才)[1] Jin Li(李瑾)[32] K. Li(李康)[13] K. Li(李科)[33] Lei Li(李蕾)[3] P. R. Li(李培荣)[41] T. Li(李腾)[33] W. D. Li(李卫东)[1] W. G. Li(李卫国)[1] X. L. Li(李晓玲)[33] X. M. Li(李小梅)[12] X. N. Li(李小男)[1,a] X. Q. Li(李学潜)[30] Z. B. Li(李志兵)[38] H. Liang(梁昊)[46,a] Y. F. Liang(梁勇飞)[36] Y. T. Liang(梁羽铁)[24] G. R. Liao(廖广睿)[11] D. X. Lin(lin)[14] B. J. Liu(刘北江)[1] C. X. Liu(刘春秀)[1] D. Liu(刘栋)[46,a] F. H. Liu(刘福虎)[35] Fang Liu(刘芳)[1] Feng Liu(刘峰)[6] H. B. Liu(刘宏邦)[12] H. H. Liu(刘欢欢)[1] H. H. Liu(刘汇慧)[16] H. M. Liu(刘怀民)[1] J. Liu(刘杰)[1] J. B. Liu(刘建北)[46,a] J. P. Liu(刘觉平)[51] J. Y. Liu(刘晶译)[1] K. Liu(刘凯)[39] K. Y. Liu(刘魁勇)[27] L. D. Liu(刘兰雕)[31] P. L. Liu(刘佩莲)[1,a] Q. Liu(刘倩)[41] S. B. Liu(刘树彬)[46,a] X. Liu(刘翔)[26] Y. B. Liu(刘玉斌)[30] Z. A. Liu(刘振安)[1,a] Zhiqing Liu(刘智清)[22] H. Loehner[25] X. C. Lou(娄辛丑)[1,a,h] H. J. Lu(吕海江)[17] J. G. Lu(吕军光)[1,a] Y. Lu(卢宇)[1] Y. P. Lu(卢云鹏)[1,a] C. L. Luo(罗成林)[28] M. X. Luo(罗民兴)[52] T. Luo[42] X. L. Luo(罗小兰)[1,a] X. R. Lyu(吕晓睿)[41] F. C. Ma(马凤才)[27] H. L. Ma(马海龙)[1] L. L. Ma(马连良)[33] Q. M. Ma(马秋梅)[1] T. Ma(马天)[1] X. N. Ma(马旭

Received 11 November 2015, Revised 4 February 2016

∗ Supported by National Key Basic Research Program of China (2015CB856700), National Natural Science Foundation of China (11125525, 11235011, 11322544, 11335008, 11425524, Y61137005C), Chinese Academy of Sciences (CAS) Large-Scale Scientific Facility Program, CAS Center for Excellence in Particle Physics (CCEPP), Collaborative Innovation Center for Particles and Interactions (CICPI), Joint Large-Scale Scientific Facility Funds of NSFC and CAS (11179007, U1232201, U1332201), CAS (KJCX2-YW-N29, KJCX2-YW-N45), 100 Talents Program of CAS, National 1000 Talents Program of China, INPAC and Shanghai Key Laboratory for Particle Physics and Cosmology, German Research Foundation DFG (Collaborative Research Center CRC-1044), Istituto Nazionale di Fisica Nucleare, Italy, Ministry of Development of Turkey (DPT2006K-120470), Russian Foundation for Basic Research (14-07-91152), Swedish Research Council, U. S. Department of Energy (DE-FG02-04ER41291, DE-FG02-05ER41374, DE-FG02-94ER40823, DESC0010118), U.S. National Science Foundation, University of Groningen (RuG) and Helmholtzzentrum fuer Schwerionenforschung GmbH (GSI), Darmstadt, WCU Program of National Research Foundation of Korea (R32-2008-000-10155-0).

宁)[30] X. Y. Ma(马骁妍)[1,a] F. E. Maas[14] M. Maggiora[49A,49C] Y. J. Mao(冒亚军)[31] Z. P. Mao(毛泽普)[1] S. Marcello[49A,49C] J. G. Messchendorp[25] J. Min(闵建)[1,a] R. E. Mitchell[19] X. H. Mo(莫晓虎)[1,a] Y. J. Mo(莫玉俊)[6] C. Morales Morales[14] K. Moriya[19] N. Yu. Muchnoi[9,f] H. Muramatsu[43] Y. Nefedov[23] F. Nerling[14] I. B. Nikolaev[9,f] Z. Ning(宁哲)[1,a] S. Nisar[8] S. L. Niu(牛顺利)[1,a] X. Y. Niu(牛讯伊)[1] S. L. Olsen(馬鹏)[32] Q. Ouyang(欧阳群)[1,a] S. Pacetti[20B] Y. Pan(潘越)[46,a] P. Patteri[20A] M. Pelizaeus[4] H. P. Peng(彭海平)[46,a] K. Peters[10] J. Pettersson[50] J. L. Ping(平加伦)[28] R. G. Ping(平荣刚)[1] R. Poling[43] V. Prasad[1] M. Qi(祁鸣)[29] S. Qian(钱森)[1,a] C. F. Qiao(乔从丰)[41] L. Q. Qin(秦丽清)[33] N. Qin(覃拈)[51] X. S. Qin(秦小帅)[1] Z. H. Qin(秦中华)[1,a] J. F. Qiu(邱进发)[1] K. H. Rashid[48] C. F. Redmer[22] M. Ripka[22] G. Rong(荣刚)[1] Ch. Rosner[14] X. D. Ruan(阮向东)[12] V. Santoro[21A] A. Sarantsev[23,g] M. Savrié[21B] K. Schoenning[50] S. Schumann[22] W. Shan(单葳)[31] M. Shao(邵明)[46,a] C. P. Shen(沈成平)[2] P. X. Shen(沈培迅)[30] X. Y. Shen(沈肖雁)[1] H. Y. Sheng(盛华义)[1] W. M. Song(宋维民)[1] X. Y. Song(宋欣颖)[1] S. Sosio[49A,49C] S. Spataro[49A,49C] G. X. Sun(孙功星)[1] J. F. Sun(孙俊峰)[15] S. S. Sun(孙胜森)[1] Y. J. Sun(孙勇杰)[46,a] Y. Z. Sun(孙永昭)[1] Z. J. Sun(孙志嘉)[1,a] Z. T. Sun(孙振田)[19] C. J. Tang(唐昌建)[36] X. Tang(唐晓)[1] I. Tapan[40C] E. H. Thorndike[44] M. Tiemens[25] M. Ullrich[24] I. Uman[40B] G. S. Varner[42] B. Wang(王斌)[30] D. Wang(王东)[31] D. Y. Wang(王大勇)[31] K. Wang(王科)[1,a] L. L. Wang(王亮亮)[1] L. S. Wang(王灵淑)[1] M. Wang(王萌)[33] P. Wang(王平)[1] P. L. Wang(王佩良)[1] S. G. Wang(王思广)[31] W. Wang(王炜)[1,a] W. P. Wang(王维平)[46,a] X. F. Wang(王雄飞)[39] Y. D. Wang(王雅迪)[14] Y. F. Wang(王贻芳)[1,a] Y. Q. Wang(王亚乾)[22] Z. Wang(王铮)[1,a] Z. G. Wang(王志刚)[1,a] Z. H. Wang(王志宏)[46,a] Z. Y. Wang(王至勇)[1] T. Weber[22] D. H. Wei(魏代会)[11] J. B. Wei(韦江波)[31] P. Weidenkaff[22] S. P. Wen(文硕频)[1] U. Wiedner[4] M. Wolke[50] L. H. Wu(伍灵慧)[1] Z. Wu(吴智)[1,a] L. Xia(夏磊)[46,a] L. G. Xia(夏力钢)[39] Y. Xia(夏宇)[18] D. Xiao(肖栋)[1] H. Xiao(肖浩)[47] Z. J. Xiao(肖振军)[28] Y. G. Xie(谢宇广)[1,a] Q. L. Xiu(修青磊)[1,a] G. F. Xu(许国发)[1] L. Xu(徐雷)[1] Q. J. Xu(徐庆君)[13] X. P. Xu(徐新平)[37] L. Yan(严亮)[49A,49C] W. B. Yan(鄢文标)[46,a] W. C. Yan(闫文成)[46,a] Y. H. Yan(颜永红)[18] H. J. Yang(杨海军)[34] H. X. Yang(杨洪勋)[1] L. Yang(杨柳)[51] Y. Yang(杨迎)[6] Y. X. Yang(杨永栩)[11] M. Ye(叶梅)[1,a] M. H. Ye(叶铭汉)[7] J. H. Yin(殷俊昊)[1] B. X. Yu(俞伯祥)[1,a] C. X. Yu(喻纯旭)[30] J. S. Yu(俞洁晟)[26] C. Z. Yuan(苑长征)[1] W. L. Yuan(袁文龙)[29] Y. Yuan(袁野)[1] A. Yuncu[40B,c] A. A. Zafar[48] A. Zallo[20A] Y. Zeng(曾云)[18] Z. Zeng(曾哲)[46,a] B. X. Zhang(张丙新)[1] B. Y. Zhang(张炳云)[1,a] C. Zhang(张弛)[29] C. C. Zhang(张长春)[1] D. H. Zhang(张达华)[1] H. H. Zhang(张宏浩)[38] H. Y. Zhang(章红宇)[1,a] J. J. Zhang(张佳佳)[1] J. L. Zhang(张杰磊)[1] J. Q. Zhang(张敬庆)[1] J. W. Zhang(张家文)[1,a] J. Y. Zhang(张建勇)[1] J. Z. Zhang(张景芝)[1] K. Zhang(张坤)[1] L. Zhang(张磊)[1] X. Y. Zhang(张学尧)[33] Y. Zhang(张瑶)[1] Y. N. Zhang(张宇宁)[41] Y. H. Zhang(张银鸿)[1,a] Y. T. Zhang(张亚腾)[46,a] Yu Zhang(张宇)[41] Z. H. Zhang(张正好)[6] Z. P. Zhang(张子平)[46] Z. Y. Zhang(张振宇)[51] G. Zhao(赵光)[1] J. W. Zhao(赵京伟)[1,a] J. Y. Zhao(赵静宜)[1] J. Z. Zhao(赵京周)[1,a] Lei Zhao(赵雷)[46,a] Ling Zhao(赵玲)[1] M. G. Zhao(赵明刚)[30] Q. Zhao(赵强)[1] Q. W. Zhao(赵庆旺)[1] S. J. Zhao(赵书俊)[53] T. C. Zhao(赵天池)[1] Y. B. Zhao(赵豫斌)[1,a] Z. G. Zhao(赵政国)[46,a] A. Zhemchugov[23,d] B. Zheng(郑波)[47] J. P. Zheng(郑建平)[1,a] W. J. Zheng(郑文静)[33] Y. H. Zheng(郑阳恒)[41] B. Zhong(钟彬)[28] L. Zhou(周莉)[1,a] X. Zhou(周详)[51] X. K. Zhou(周晓康)[46,a] X. R. Zhou(周小蓉)[46,a] X. Y. Zhou(周兴玉)[1] K. Zhu(朱凯)[1] K. J. Zhu(朱科军)[1,a] S. Zhu(朱帅)[1] S. H. Zhu(朱世海)[45] X. L. Zhu(朱相雷)[39] Y. C. Zhu(朱莹春)[46,a] Y. S. Zhu(朱永生)[1] Z. A. Zhu(朱自安)[1] J. Zhuang(庄建)[1,a] L. Zotti[49A,49C] B. S. Zou(邹冰松)[1] J. H. Zou(邹佳恒)[1]

(BESIII Collaboration)

[1] Institute of High Energy Physics, Beijing 100049, China
[2] Beihang University, Beijing 100191, China
[3] Beijing Institute of Petrochemical Technology, Beijing 102617, China
[4] Bochum Ruhr-University, D-44780 Bochum, Germany
[5] Carnegie Mellon University, Pittsburgh, Pennsylvania 15213, USA
[6] Central China Normal University, Wuhan 430079, China
[7] China Center of Advanced Science and Technology, Beijing 100190, China
[8] COMSATS Institute of Information Technology, Lahore, Defence Road, Off Raiwind Road, 54000 Lahore, Pakistan
[9] G.I. Budker Institute of Nuclear Physics SB RAS (BINP), Novosibirsk 630090, Russia
[10] GSI Helmholtzcentre for Heavy Ion Research GmbH, D-64291 Darmstadt, Germany
[11] Guangxi Normal University, Guilin 541004, China
[12] GuangXi University, Nanning 530004, China
[13] Hangzhou Normal University, Hangzhou 310036, China
[14] Helmholtz Institute Mainz, Johann-Joachim-Becher-Weg 45, D-55099 Mainz, Germany
[15] Henan Normal University, Xinxiang 453007, China
[16] Henan University of Science and Technology, Luoyang 471003, China
[17] Huangshan College, Huangshan 245000, China
[18] Hunan University, Changsha 410082, China
[19] Indiana University, Bloomington, Indiana 47405, USA

[20] (A)INFN Laboratori Nazionali di Frascati, I-00044, Frascati, Italy; (B)INFN and University of Perugia, I-06100, Perugia, Italy
[21] (A)INFN Sezione di Ferrara, I-44122, Ferrara, Italy; (B)University of Ferrara, I-44122, Ferrara, Italy
[22] Johannes Gutenberg University of Mainz, Johann-Joachim-Becher-Weg 45, D-55099 Mainz, Germany
[23] Joint Institute for Nuclear Research, 141980 Dubna, Moscow region, Russia
[24] Justus Liebig University Giessen, II. Physikalisches Institut, Heinrich-Buff-Ring 16, D-35392 Giessen, Germany
[25] KVI-CART, University of Groningen, NL-9747 AA Groningen, The Netherlands
[26] Lanzhou University, Lanzhou 730000, China
[27] Liaoning University, Shenyang 110036, China
[28] Nanjing Normal University, Nanjing 210023, China
[29] Nanjing University, Nanjing 210093, China
[30] Nankai University, Tianjin 300071, China
[31] Peking University, Beijing 100871, China
[32] Seoul National University, Seoul, 151-747 Korea
[33] Shandong University, Jinan 250100, China
[34] Shanghai Jiao Tong University, Shanghai 200240, China
[35] Shanxi University, Taiyuan 030006, China
[36] Sichuan University, Chengdu 610064, China
[37] Soochow University, Suzhou 215006, China
[38] Sun Yat-Sen University, Guangzhou 510275, China
[39] Tsinghua University, Beijing 100084, China
[40] (A)Istanbul Aydin University, 34295 Sefakoy, Istanbul, Turkey; (B)Dogus University, 34722 Istanbul, Turkey; (C)Uludag University, 16059 Bursa, Turkey
[41] University of Chinese Academy of Sciences, Beijing 100049, China
[42] University of Hawaii, Honolulu, Hawaii 96822, USA
[43] University of Minnesota, Minneapolis, Minnesota 55455, USA
[44] University of Rochester, Rochester, New York 14627, USA
[45] University of Science and Technology Liaoning, Anshan 114051, China
[46] University of Science and Technology of China, Hefei 230026, China
[47] University of South China, Hengyang 421001, China
[48] University of the Punjab, Lahore-54590, Pakistan
[49] (A)University of Turin, I-10125, Turin, Italy; (B)University of Eastern Piedmont, I-15121, Alessandria, Italy; (C)INFN, I-10125, Turin, Italy
[50] Uppsala University, Box 516, SE-75120 Uppsala, Sweden
[51] Wuhan University, Wuhan 430072, China
[52] Zhejiang University, Hangzhou 310027, China
[53] Zhengzhou University, Zhengzhou 450001, China

[a] Also at State Key Laboratory of Particle Detection and Electronics, Beijing 100049, Hefei 230026, China
[b] Also at Ankara University,06100 Tandogan, Ankara, Turkey
[c] Also at Bogazici University, 34342 Istanbul, Turkey
[d] Also at the Moscow Institute of Physics and Technology, Moscow 141700, Russia
[e] Also at the Functional Electronics Laboratory, Tomsk State University, Tomsk, 634050, Russia
[f] Also at the Novosibirsk State University, Novosibirsk, 630090, Russia
[g] Also at the NRC "Kurchatov Institute", PNPI, 188300, Gatchina, Russia
[h] Also at University of Texas at Dallas, Richardson, Texas 75083, USA
[i] Also at Istanbul Arel University, 34295 Istanbul, Turkey

**Abstract:** From 2011 to 2014, the BESIII experiment collected about 5 $\mathrm{fb}^{-1}$ data at center-of-mass energies around 4 GeV for the studies of the charmonium-like and higher excited charmonium states. By analyzing the di-muon process $\mathrm{e^+e^-} \to \gamma_{\mathrm{ISR/FSR}}\mu^+\mu^-$, the center-of-mass energies of the data samples are measured with a precision of 0.8 MeV. The center-of-mass energy is found to be stable for most of the time during data taking.

**Keywords:** center-of-mass energy, di-muon process, charmoniumlike states

**PACS:** 06.30.-k, 13.66.Jn **DOI:** 10.1088/1674-1137/40/6/063001

## 1 Introduction

The BESIII detector operating at the BEPCII accelerator is designed to study physics in the $\tau$-charm energy region (2–4.6 GeV) [1]. From 2011 to 2014, the BESIII experiment accumulated 5 $\mathrm{fb}^{-1}$ of $\mathrm{e^+e^-}$ collision data at center-of-mass energies between 3.810 and 4.600 GeV to study the charmonium-like and higher excited charmonium states [2]. In the past, BESIII has taken large data samples at the J/$\psi$, $\psi(3686)$ and $\psi(3770)$ peaks. The corresponding beam energy was fine tuned by a J/$\psi$ or $\psi(3686)$ mass scan before the data-taking. However, around 4 GeV, there is no narrow resonance in $\mathrm{e^+e^-}$ annihilation, and the $\psi(3686)$ peak is too far away to be used to calibrate the beam energy. The Beam Energy Measurement System (BEMS), which was installed in

2008, is designed to measure the beam energy with a relative systematic uncertainty of $2\times10^{-5}$ [3] based on the energies of Compton back-scattered photons. The performance of BEMS is verified through measurement of the $\psi(3686)$ mass, but 4 GeV is beyond the working range of BEMS. To precisely measure the masses of the newly observed $Z_c$ [4, 5] particles, especially for those which are observed by a partial reconstruction method [6, 7], a precise knowledge of the center-of-mass energy ($E_{\rm cms}$) is crucial.

In this paper, we develop a method to measure the $E_{\rm cms}$ using the di-muon process

$$e^+e^- \to (\gamma_{\rm ISR/FSR})\mu^+\mu^-, \quad (1)$$

where $\gamma_{\rm ISR/FSR}$ represents possible initial state radiative (ISR) or final state radiative (FSR) photons. The $E_{\rm cms}$ can be written as

$$E_{\rm cms} = M(\mu^+\mu^-) + \Delta M_{\rm ISR/FSR}, \quad (2)$$

where $M(\mu^+\mu^-)$ is the invariant mass of $\mu^+\mu^-$, and $\Delta M_{\rm ISR/FSR}$ is the mass shift due to ISR/FSR radiation. In the analysis, $\Delta M_{\rm ISR/FSR}$ is estimated from a Monte Carlo (MC) simulation of the di-muon process by turning the ISR/FSR on or off, where the ISR/FSR is simulated by BABAYAGA3.5 [8]. To make sure the measured invariant mass $M(\mu^+\mu^-)$ is unbiased, we validate the reconstructed momentum of $\mu^+/\mu^-$ with the $J/\psi$ signal from the process $e^+e^- \to \gamma_{\rm ISR}J/\psi$ with $J/\psi \to \mu^+\mu^-(\gamma_{\rm FSR})$ in the same data samples.

## 2 The BESIII detector and data sets

The BESIII detector is described in detail in Ref. [9]. The detector is cylindrically symmetric and covers 93% of the solid angle around the collision point. The detector consists of four main components: (a) A 43-layer main drift chamber (MDC) provides momentum measurement for charged tracks with a momentum resolution of 0.5% at 1 GeV/$c$ in a 1 T magnetic field. (b) A time-of-flight system (TOF) composed of plastic scintillators has a time resolution of 80 ps (110 ps) in the barrel (endcaps). (c) An electromagnetic calorimeter (EMC) made of 6240 CsI(Tl) crystals provides an energy resolution for photons of 2.5% (5%) at 1 GeV in the barrel (endcaps). (d) A muon counter (MUC), consisting of 9 (8) layers of resistive plate chambers in the barrel (endcaps) within the return yoke of the magnet, provides 2 cm position resolution. The electron and positron beams collide with an angle of 22 mrad at the interaction point (IP) in order to separate the $e^+$ and $e^-$ beams after the collision. A GEANT4 [10] based detector simulation package is developed to model the detector response for MC events.

In total, there are 25 data samples taken at different center-of-mass energies or during different periods, as listed in Table 1. The data sets are listed chronologically, and the ID number is the requested $E_{\rm cms}$. The offline luminosity is measured through large-angle Bhabha scattering events with a precision of 1% [11]. In this paper, we measure $E_{\rm cms}$ for all the 25 data samples and examine its stability during each data taking period.

## 3 Muon momentum validation with $J/\psi$ signal

The measurement of high momentum muons is validated with $J/\psi \to \mu^+\mu^-$ candidates selected via the process $e^+e^- \to \gamma_{\rm ISR}J/\psi$. Events must have only two good oppositely charged tracks. Each good charged track must be consistent with originating from the IP, by requiring the impact parameter to be within 1 cm in the radial direction ($V_{xy} < 1$ cm) and 10 cm in the $z$ direction ($|V_z| < 10$ cm) from the run-dependent IP, and within the polar angle region $|\cos\theta| < 0.8$ (i.e. accepting only tracks in the barrel region). The energy deposition in the EMC ($E$) for each charged track is required to be less than 0.4 GeV to suppress background from radiative Bhabha events. A further requirement on the opening angle between the two tracks, $\cos\theta_{\mu^+\mu^-} > -0.98$, is used to remove cosmic rays. The background remaining after the above selection comes from the radiative di-muon process, which has exactly the same final state and cannot be completely removed. The radiative di-muon events show a smooth distribution in $M(\mu^+\mu^-)$. With the above selection criteria imposed, the distribution of $M(\mu^+\mu^-)$ of each sample, having a tail on the low mass side due to final state radiation (FSR) effects, is fitted with an asymmetric function of a crystal-ball function [12] for the $J/\psi$ signal and a linear function to model the background. Figure 1 shows the fit result for data sample 4600 as an example. In order to reduce the fluctuation of $M(\mu^+\mu^-)$, adjacent data samples with small statistics are combined. Due to FSR, $J/\psi \to \mu^+\mu^-\gamma_{\rm FSR}$, the measured $M^{\rm obs}(\mu^+\mu^-)$ is slightly lower than the nominal $J/\psi$ mass [13]. The mass shift due to the FSR photon(s) $\Delta M_{\rm FSR}$ is estimated by simulated samples of the process $e^+e^- \to \gamma_{\rm ISR}J/\psi$ with 50,000 events each, generated at different energies using the generator PHOTOS [15] with FSR turned on and off. The mass shift $\Delta M_{\rm FSR}$ at each $E_{\rm cms}$ is obtained as the difference in $M^{\rm obs}(\mu^+\mu^-)$ between the MC samples with FSR turned on and off. These simulation studies validate that $\Delta M_{\rm FSR}$ is independent of $E_{\rm cms}$. A weighted average, $\overline{\Delta M}_{\rm FSR} = (0.59 \pm 0.04)$ MeV/$c^2$, is obtained by fitting the $\Delta M_{\rm FSR}$ versus $E_{\rm cms}$. The measured mass corrected by $\overline{\Delta M}_{\rm FSR}$, $M^{\rm cor}(\mu^+\mu^-)$, is plotted in Fig. 2 and listed in Table 1 (column 4). The values of $M^{\rm cor}(\mu^+\mu^-)$ for the different data samples are consistent within errors. By fitting the $M^{\rm cor}(\mu^+\mu^-)$ of all data samples with

a first-order polynomial, the average $\overline{M}^{\rm cor}(\mu^+\mu^-)$ is obtained to be $\overline{M}^{\rm cor}(\mu^+\mu^-) = 3096.79\pm0.08\,{\rm MeV}/c^2$, which agrees with the nominal J/ψ mass within errors. The goodness of the fit is $\chi^2/ndf = 11.68/11 = 1.06$. The small difference is considered as a systematic uncertainty in Section 7.

Table 1. Summary of the data sets, including ID, run number, offline luminosity, the measured $M^{\rm cor}({\rm J/\psi})$, $M^{\rm obs}(\mu^+\mu^-)$, and $E_{\rm cms}$. The first uncertainty is statistical, and the second is systematic. Superscripts indicate separate samples acquired at the same $E_{\rm cms}$. The "-" indicates samples which are combined with the previous one(s) to measure $M^{\rm cor}(\mu^+\mu^-)$.

| ID | run number | offline lum./pb$^{-1}$ | $M^{\rm cor}({\rm J/\psi})/({\rm MeV}/c^2)$ | $M^{\rm obs}(\mu^+\mu^-)/({\rm MeV}/c^2)$ | $E_{\rm cms}$/MeV |
|---|---|---|---|---|---|
| 4009[1] | 23463 to 23505 | 481.96±0.01 | 3097.00±0.15 | 4005.90±0.15 | 4009.10±0.15±0.59 |
| 4009[2] | 23510 to 24141 | | – | 4004.26±0.05 | 4007.46±0.05±0.66 |
| 4260[1] | 29677 to 29805 | 523.74±0.10 | 3096.95±0.26 | (4367.37−3.75×$10^{-3}\times N_{\rm run}$)±0.12 | (4370.95−3.75×$10^{-3}\times N_{\rm run}$)±0.12±0.62 |
| 4260[2] | 29822 to 30367 | | – | 4254.42±0.06 | 4258.00±0.06±0.60 |
| 4190 | 30372 to 30437 | 43.09±0.03 | 3097.53±0.51 | 4185.12±0.15 | 4188.59±0.15±0.68 |
| 4230[1] | 30438 to 30491 | 44.40±0.03 | – | 4223.83±0.18 | 4227.36±0.18±0.63 |
| 4310 | 30492 to 30557 | 44.90±0.03 | – | 4304.22±0.17 | 4307.89±0.17±0.63 |
| 4360 | 30616 to 31279 | 539.84±0.10 | 3096.42±0.28 | 4354.51±0.05 | 4358.26±0.05±0.62 |
| 4390 | 31281 to 31325 | 55.18±0.04 | 3096.39±0.62 | 4383.60±0.17 | 4387.40±0.17±0.65 |
| 4420[1] | 31327 to 31390 | 44.67±0.03 | – | 4413.10±0.20 | 4416.95±0.20±0.63 |
| 4260[3] | 31561 to 31981 | 301.93±0.08 | 3096.76±0.34 | 4253.85±0.07 | 4257.43±0.07±0.66 |
| 4210 | 31983 to 32045 | 54.55±0.03 | 3096.88±0.43 | 4204.23±0.14 | 4207.73±0.14±0.61 |
| 4220 | 32046 to 32140 | 54.13±0.03 | – | 4213.61±0.14 | 4217.13±0.14±0.67 |
| 4245 | 32141 to 32226 | 55.59±0.04 | – | 4238.10±0.12 | 4241.66±0.12±0.73 |
| 4230[2] | 32239 to 32849 | 1047.34±0.14 | 3096.58±0.18 | (4316.81−2.87×$10^{-3}\times N_{\rm run}$)±0.05 | (4320.34−2.87×$10^{-3}\times N_{\rm run}$)±0.05±0.60 |
| 4230[3] | 32850 to 33484 | | – | 4222.01±0.05 | 4225.54±0.05±0.65 |
| 3810 | 33490 to 33556 | 50.54±0.03 | 3097.38±0.37 | 3804.82±0.10 | 3807.65±0.10±0.58 |
| 3900 | 33572 to 33657 | 52.61±0.03 | – | 3893.26±0.11 | 3896.24±0.11±0.72 |
| 4090 | 33659 to 33719 | 52.63±0.03 | – | 4082.15±0.14 | 4085.45±0.14±0.66 |
| 4600 | 35227 to 36213 | 566.93±0.11 | 3096.54±0.33 | 4595.38±0.07 | 4599.53±0.07±0.74 |
| 4470 | 36245 to 36393 | 109.94±0.04 | 3096.69±0.42 | 4463.13±0.11 | 4467.06±0.11±0.73 |
| 4530 | 36398 to 36588 | 109.98±0.04 | – | 4523.10±0.11 | 4527.14±0.11±0.72 |
| 4575 | 36603 to 36699 | 47.67±0.03 | – | 4570.39±0.18 | 4574.50±0.18±0.70 |
| 4420[2] | 36773 to 37854 | 1028.89±0.13 | 3096.65±0.21 | 4411.99±0.04 | 4415.84±0.04±0.62 |
| 4420[3] | 37855 to 38140 | | – | 4410.21±0.07 | 4414.06±0.07±0.72 |

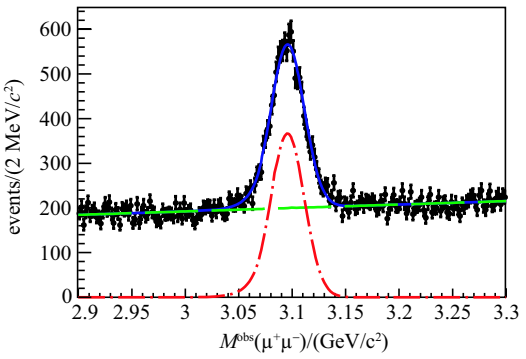


Fig. 1. (color online) Fit to the $M^{\rm obs}(\mu^+\mu^-)$ distribution in $e^+e^-\to\gamma_{\rm ISR}{\rm J/\psi}$ events for one data sample. Black dots with error bars are data, the blue curve shows the fit result, the red dash-dotted curve is for signal, and the green dashed line is for background.

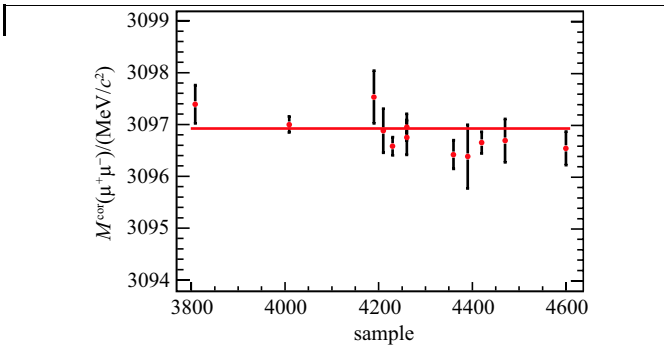


Fig. 2. (color online) Measured J/ψ mass after the FSR correction, $M^{\rm cor}(\mu^+\mu^-)$, for data taken at different energies, in which the data samples with small statistics are merged (described in text). The red solid line is the nominal J/ψ mass for reference.

## 4 The mass shift $\Delta M_{\rm ISR/FSR}$

The $E_{\rm cms}$ of the initial $e^+e^-$ pair is measured via the di-muon process $e^+e^- \to \gamma_{\rm ISR/FSR}\mu^+\mu^-$. However, due to the emission of radiative photons, the invariant mass of the $\mu^+\mu^-$ pair is less than the $E_{\rm cms}$ of the initial $e^+e^-$ pair by $\Delta M_{\rm ISR/FSR}$. In general, the mass shift due to FSR is small, about 0.6 MeV/$c^2$ at 3.097 GeV, and the mass shift due to ISR is 2–3 MeV/$c^2$, which has been well studied theoretically [14]. In the analysis, the $\Delta M_{\rm ISR/FSR}$ is estimated with MC simulation using BABAYAGA3.5 [8]. We generate 50000 di-muon MC events for each sample with ISR/FSR turned on and off, and take the difference in $M(\mu^+\mu^-)$ as the mass shift $\Delta M_{\rm ISR/FSR}$ caused by ISR and FSR. In order to avoid possible bias, the same event selection criteria for the di-muon process applied for data (as described in Section 5) are imposed to the MC samples.

The distributions of $M(\mu^+\mu^-)$ with ISR/FSR on and off are fitted with a Gaussian function in a range around the peak (same method with data in Section 5). The difference in peak positions (the mass shift $\Delta M_{\rm ISR/FSR}$) versus $E_{\rm cms}$ is seen to increase with $E_{\rm cms}$, as shown in Fig. 3. The $\Delta M_{\rm ISR/FSR}$ is fitted with a linear function. The fit result is $\overline{\Delta M}_{\rm ISR/FSR} = (-3.53 \pm 1.11) + (1.67 \pm 0.28) \times 10^{-3} \times E_{\rm cms}/{\rm MeV}$ with statistical uncertainty only. The goodness of the fit is $\chi^2/n.d.f = 6.3/13$. The resulting $E_{\rm cms}$-dependent $\overline{\Delta M}_{\rm ISR/FSR}$ will be used to correct the measured $M^{\rm obs}(\mu^+\mu^-)$ for the effects of ISR and FSR.

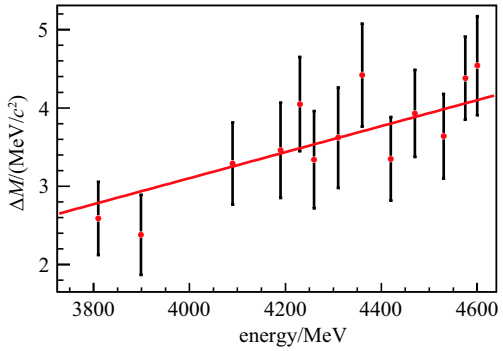


Fig. 3. (color online) Difference in $M^{\rm obs}(\mu^+\mu^-)$ between the MC samples with ISR/FSR turned on and off (the mass shift $\Delta M_{\rm ISR/FSR}$) versus center-of-mass energy for $e^+e^- \to \gamma_{\rm ISR/FSR}\mu^+\mu^-$ MC samples. The red solid line is the fit result.

The mass shift due to FSR only, $\Delta M_{\rm FSR}$, is estimated by comparing MC samples of di-muon production with FSR turned on and off. We find that $\Delta M_{\rm FSR}$ increases with $E_{\rm cms}$ and we parameterize the $E_{\rm cms}$ dependence with a first-order polynomial as $\overline{\Delta M}_{\rm FSR} = (-1.34\pm0.84)+(0.56\pm0.21)\times10^{-3}\times E_{\rm cms}/{\rm MeV}$, where the corresponding correlation coefficient between the parameters is -0.964. So the corresponding $\Delta M_{\rm FSR}$ at 3.81 GeV (4.6 GeV) is 0.79±0.09 MeV/$c^2$ (1.24±0.14 MeV/$c^2$).

## 5 The measurement of $E_{\rm cms}$

To select the di-muon process $e^+e^- \to (\gamma_{\rm ISR/FSR})\mu^+\mu^-$, the requirement for charged tracks is the same as the $\gamma_{\rm ISR}J/\psi$ selection. To achieve the best precision, only events with both tracks in the barrel region (i.e., in the polar angle region $|\cos\theta| < 0.80$) are accepted. A requirement on the opening angle between the two tracks of $178.60^\circ < \theta_{\mu\mu} < 179.64^\circ$ is applied to suppress cosmic ray and di-muon events with high-energy radiative photons. To further remove cosmic ray events, the TOF timing difference between the two tracks is required to be $|\Delta t| < 4$ ns. The background contribution following the above selection criteria is less than 0.001% compared to signal and is therefore neglected in the following.

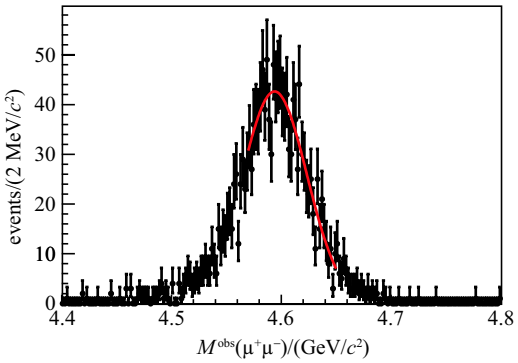


Fig. 4. (color online) Fit to the $M^{\rm obs}(\mu^+\mu^-)$ distribution for a run. Black dots with error bars are data, and the red curve shows the fit result.

After applying the above selection, the distribution of $M^{\rm obs}(\mu^+\mu^-)$ for selected di-muon events has a tail in the low mass side which cannot be described by a single Gaussian. Since only the peak position of the distribution will be used, we estimate it by fitting with a Gaussian function in the range of $(-1\sigma, 2\sigma)$ around the peak, where $\sigma$ is the standard deviation of the Gaussian. To examine the stability of $E_{\rm cms}$ over time for each data sample, the fit procedure is performed for each run of the data samples, where a run normally corresponds to one hour of data taking. The fit result for one run of the 4600 data sample is shown in Fig. 4. The measured $\mu^+\mu^-$ masses versus the run number for the samples $4009^{1,2}$, $4260^{1,2}$, 4360, $4230^{2,3}$, 4600, and $4420^{2,3}$ are plotted in Fig. 5. For the sample $4260^1$ ($4230^2$), the measured $M^{\rm obs}(\mu^+\mu^-)$ changes slowly and is fitted with a linear function. The fit gives $(4367.37 \pm 53.53) + (-3.75 \pm 1.80) \times 10^{-3} \times N_{\rm run}$ $((4316.81\pm7.84)+(-2.87\pm0.24)\times10^{-3}\times N_{\rm run})$ in unit of MeV/$c^2$, where $N_{\rm run}$ is the run number. Since the uncertainty is $N_{\rm run}$ dependent, we take the largest value from error propagation as the corresponding statistical uncertainty. For other data samples, $M^{\rm obs}(\mu^+\mu^-)$ remains

stable, and the average value is used to calculate $E_{\rm cms}$. The samples $4009^1$ ($4420^2$) and $4009^2$ ($4420^3$) are separated because they show a sudden drop in the average energies. Table 1 (column 5) summarizes the measured $M^{\rm obs}(\mu^+\mu^-)$ for each sample.

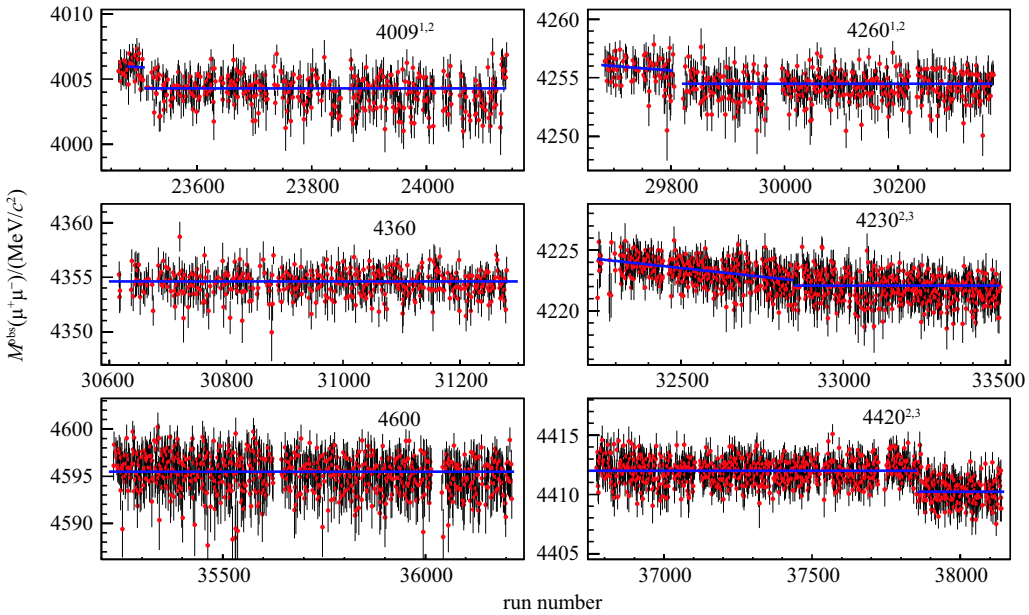


Fig. 5. (color online) Measured $M^{\rm obs}(\mu^+\mu^-)$ of di-muon events run-by-run for samples $4009^{1,2}$, $4260^{1,2}$, 4360, $4230^{2,3}$, 4600, and $4420^{2,3}$. The blue solid lines show the fit results for the data samples.

$E_{\rm cms}$ is finally obtained by adding the energy-dependent mass shift $\overline{\Delta M}_{\rm ISR/FSR}$ due to ISR/FSR obtained in Section 4 to the measured $M^{\rm obs}(\mu^+\mu^-)$. The measured $E_{\rm cms}$ is listed in Table 1 (column 6); the systematic uncertainty will be discussed in Section 7.

Each of the data sets 4009, 4230, 4260, and 4420 is split into several sub-samples. We calculate the luminosity-weighted average $E_{\rm cms}$ for each, and the largest systematic uncertainty of the sub-samples is taken as the systematic uncertainty. In Table 2, we summarize the weighted average $E_{\rm cms}$ for all data samples.

Table 2. Weighted average $E_{\rm cms}$ for all data samples. The first uncertainty is statistical, and the second is systematic.

| ID | weighted average $E_{\rm cms}$/MeV |
|---|---|
| 3810 | 3807.65±0.10±0.58 |
| 3900 | 3896.24±0.11±0.72 |
| 4009 | 4007.62±0.05±0.66 |
| 4090 | 4085.45±0.14±0.66 |
| 4190 | 4188.59±0.15±0.68 |
| 4210 | 4207.73±0.14±0.61 |
| 4220 | 4217.13±0.14±0.67 |
| 4230 | 4226.26±0.04±0.65 |
| 4245 | 4241.66±0.12±0.73 |
| 4260 | 4257.97±0.04±0.66 |
| 4310 | 4307.89±0.17±0.63 |
| 4360 | 4358.26±0.05±0.62 |
| 4390 | 4387.40±0.17±0.65 |
| 4420 | 4415.58±0.04±0.72 |
| 4470 | 4467.06±0.11±0.73 |
| 4530 | 4527.14±0.11±0.72 |
| 4575 | 4574.50±0.18±0.70 |
| 4600 | 4599.53±0.07±0.74 |

## 6 Cross check

The processes of $e^+e^- \to \pi^+\pi^-K^+K^-$ and $e^+e^- \to \pi^+\pi^-p\bar{p}$ are used to check the measurement of $E_{\rm cms}$. Similar to the di-muon process $e^+e^- \to \gamma_{\rm ISR/FSR}\mu^+\mu^-$, the $E_{\rm cms}$ of the initial $e^+e^-$ system is estimated by the corrected invariant masses of the final state particles $M^{\rm cor}(\pi^+\pi^-K^+K^-)$ and $M^{\rm cor}(\pi^+\pi^-p\bar{p})$. The measurement of the low momentum charged tracks is validated using the decay channels $D^0 \to K^-\pi^+$ and $\bar{D}^0 \to K^+\pi^-$. The measured mass, $M^{\rm obs}(K^-\pi^+/K^+\pi^-) = 1864.00 \pm 0.70$ MeV/$c^2$ (statistical uncertainty only) is consistent with the nominal $D^0/\bar{D}^0$ mass [13] with a deviation of $0.84 \pm 0.71$ MeV/$c^2$. Both the corrected $M^{\rm cor}(\pi^+\pi^-K^+K^-)$ and $M^{\rm cor}(\pi^+\pi^-p\bar{p})$ are found to be consistent with $E_{\rm cms}$ obtained using the di-muon process, with the largest deviation of 0.53±0.75 MeV found in sample 4420.

## 7 Systematic uncertainties

The systematic uncertainty in $E_{\rm cms}$ in this analysis is estimated by considering the uncertainties from the momentum measurement of the $\mu^{\pm}$, the estimation of the mass shift $\Delta M_{\rm ISR/FSR}$ due to ISR/FSR, the generator, and the corresponding fit procedure.

We use the $J/\psi$ invariant mass via the process $J/\psi \to \mu^+\mu^-$ to check the momentum reconstruction. The measured $J/\psi$ mass corrected for FSR effects at each energy, $M^{\rm cor}(J/\psi)$, is close to the nominal $J/\psi$ mass. To be conservative, we use a first-order polynomial to fit the $M^{\rm cor}(J/\psi)$ versus $E_{\rm cms}$ distribution, and find the largest difference in the $J/\psi$ mass between the fit result and the nominal value to be 0.34 MeV/$c^2$. We take $\frac{0.34}{3096.92} = 0.011\%$ as the systematic uncertainty due to the momentum measurement.

The mass shift $\Delta M_{\rm ISR/FSR}$ due to ISR/FSR is $E_{\rm cms}$ dependent, and is obtained from MC samples with 50,000 generated events each. The standard deviation of the distribution of $\Delta M_{\rm ISR/FSR}$ versus $E_{\rm cms}$ is given by

$$\sigma = \sqrt{\frac{\Sigma(\Delta M_{\rm ISR/FSR} - \overline{\Delta M}_{\rm ISR/FSR})^2}{N-1}} = 0.37 \text{ MeV}/c^2, \tag{3}$$

where $\overline{\Delta M}_{\rm ISR/FSR}$ is the value from the fit (Fig. 3), and $N$ is the number of points in Fig. 3. A value of 0.37 MeV/$c^2$ is taken as systematic uncertainty due to the ISR/FSR correction.

Additionally, we use two different generators (BABAYAGA3.5 and BABAYAGA@NLO) to estimate the mass shift $\Delta M_{\rm ISR/FSR}$. The averaged difference in $\Delta M_{\rm ISR/FSR}$ from the two generators is $0.036 \pm 0.067$ MeV/$c^2$, which reflects the contribution to the systematic uncertainty of the ISR/FSR correction from the generator; it is negligibly small.

$M^{\rm obs}(\mu^+\mu^-)$ is measured run-by-run and is found to be stable during data-taking for most samples. For the runs in each sample (except for samples 4230[2] and 4260[1], which are described by a first-order polynomial), the average $E_{\rm cms}$ is provided to reduce the statistical fluctuation. If the energy shifts gradually during the data-taking, the simple average value will cause a systematic uncertainty. To estimate this systematic error for each sample, we fit the distribution of $M^{\rm obs}(\mu^+\mu^-)$ versus run-number by a first-order polynomial and take the largest difference between the fitting result and the average value, less than 0.25 MeV/$c^2$ on average, as the systematic uncertainty.

The uncertainties from other sources, such as background and event selection, are negligible. Assuming all the sources of systematic uncertainty are independent, the total systematic uncertainty is obtained by adding all items in quadrature, giving the values listed in Table 1 (column 6). The uncertainty is smaller than 0.8 MeV for all the data samples.

## 8 Summary

The center-of-mass energies of the data taken from 2011 to 2014 for the studies of the charmonium-like and higher excited charmonium states are measured with the di-muon process $e^+e^- \to (\gamma_{\rm ISR/FSR})\mu^+\mu^-$. The corresponding statistical uncertainty is very small, and the systematic uncertainty is found to be less than 0.8 MeV. The measured $E_{\rm cms}$ is validated by the processes $e^+e^- \to \pi^+\pi^-K^+K^-$ and $e^+e^- \to \pi^+\pi^-p\bar{p}$. The stability of $E_{\rm cms}$ over time for the data samples is examined. For samples 4009, 4230, 4260, 4420, we also give the luminosity-weighted average $E_{\rm cms}$. The results are essential for the discovery of new states and investigation of the transition of charmonium and charmonium-like states [4–7].

*The BESIII collaboration thanks the staff of BEPCII and the IHEP computing center for their strong support.*

## References


1 D. M. Asner et al, Int. J. Mod. Phys. A, **24**: 499 (2009)
2 N. Brambilla et al, Eur. Phys. J. C, **71**: 1534 (2011)
3 E. V. Abakumova et al, Nucl. Instrum. Methods A, **659**: 21 (2011)
4 M. Ablikim et al (BESIII Collaboration), Phys. Rev. Lett., **110**: 252001 (2013)
5 M. Ablikim et al (BESIII Collaboration), Phys. Rev. Lett., **111**: 242001 (2014)
6 M. Ablikim et al (BESIII Collaboration), Phys. Rev. Lett., **112**: 022001 (2014)
7 M. Ablikim et al (BESIII Collaboration), Phys. Rev. Lett., **112**: 132001 (2014)
8 G. Balossini, C. M. Carloni Calame, G. Montagna et al, Nucl. Phys. B, **758**: 227 (2006)
9 M. Ablikim et al (BESIII Collaboration), Nucl. Instrum. Methods A, **614**: 345 (2010)
10 S. Agostinelli et al (GEANT4 Collaboration), Nucl. Instrum. Methods A, **506**: 250 (2003)
11 M. Ablikim et al (BESIII Collaboration), Chin. Phys. C, **39**: 093001 (2015)
12 T. Skwarnicki et al, Report No. DESY F31-86-02 (1986)
13 K. A. Olive et al (Particle Data Group), Chin. Phys. C, **38**: 090001 (2014)
14 E. A. Kuraev and V. S. Fadin, Yad. Fiz. **41**: 773 (1985) (Sov. J. Nucl. Phys., **41**: 466 (1985))
15 E. Barberio and Z. Was, Comput. Phys. Commun., **79**: 291 (1994)